A highly membrane-active peptide in Flock House virus: implications for the mechanism of nodavirus infection

Dennis T Bong, Claudia Steinem, Andreas Janshoff, John E Johnson and M Reza Ghadiri

Background: Nodaviruses are among the simplest animal viruses, and are therefore attractive systems for deconvoluting core viral processes such as assembly, infection and uncoating. Membrane translocation of the single-stranded RNA genome of nodaviruses has been proposed to be mediated by direct lipid–protein interactions between a post-assembly autocatalytic cleavage product from the capsomere and the target membrane. To probe the validity of this hypothesis, we have synthesized a 21-residue Met→Nle (norleucine) variant of the amino-terminal helical domain (denoted here as γ_1) of the cleavage peptide in Flock House nodavirus (FHV) and studied its ability to alter membrane structure and function.

Results: The synthetic peptide γ_1 increases membrane permeability to hydrophilic solutes, as judged by fluorescence experiments with liposome-encapsulated dyes and ion-conductance measurements. Furthermore, peptide orientation and location within lipid bilayers was determined using tryptophan-fluorescence-quenching experiments and attenuated total reflectance infrared spectroscopy.

Conclusions: The helical domain of the FHV cleavage product partitions spontaneously into lipid bilayers and increases membrane permeability, consistent with the postulated mechanism for viral genome translocation. The existence of a membrane-binding domain in the FHV cleavage sequence suggests peptide-triggered disruption of the endosomal membrane as a prelude to viral uncoating in the host cytoplasm. A model for this interaction is proposed.

Address: Departments of Chemistry and Molecular Biology at the Scripps Research Institute and the Skaggs Institute for Chemical Biology, La Jolla, CA 92037, USA.

Correspondence: M Reza Ghadiri
E-mail: ghadiri@scripps.edu

Key words: Flock House nodavirus, γ peptide, membrane permeability, RNA translocation, transfection mechanism

Received: **25 February 1999**
Revisions requested: **14 April 1999**
Revisions received: **21 April 1999**
Accepted: **23 April 1999**

Published: **18 June 1999**

Chemistry & Biology July 1999, 6:473–481
http://biomednet.com/elecref/1074552100600473

 ISSN 1074-5521

Introduction

Nodaviruses are nonenveloped RNA animal viruses composed of a bipartite single-stranded RNA genome encoding three genes packaged within an icosahedral capsid assembly of 180 identical gene products. Genetic economy dictates relative simplicity (as well as multiplicity) of function, and elucidating the nodaviral machinery might therefore provide an elementary paradigm that can be applied to other more complex viruses [1]. It is thought that nodaviruses, in analogy to picornaviruses, enter cells via receptor-binding-induced endocytosis; virus uncoating then occurs, concomitant with passage of RNA across the endosomal membrane. Although some of the mechanistic aspects of cell entry and viral uncoating have been determined for picornaviruses such as poliovirus [2] and rhinovirus [3,4], a detailed understanding of these processes remains elusive, particularly for nodaviruses. Interestingly, the infectivity of assembled nodavirus particles is thought to be contingent upon a maturation event common to all nodaviruses, in which most of the capsid proteins autocatalytically cleave a peptide sequence from their carboxyl termini [5,6]. Although the connection between infectivity and cleavage is as yet unclear, high-resolution structural investigations of nodaviruses [7,8] and other simple RNA viruses [9] has suggested a possible role for the cleavage peptides in infectivity. The cleavage peptides remain non-covalently associated with the capsid interior and are arranged as homo-oligomeric helical bundles along the high-symmetry axes of the icosahedral capsid assembly (Figure 1). Only the amino-terminal regions of the cleavage products are visible as helices in the structural data, as the carboxy-terminal region is disordered and presumably contacting RNA. Indeed, it has been recently demonstrated [10] in Flock House nodavirus (FHV) that packaging specificity depends on sequence fidelity in the carboxy-terminal region of the 44-residue cleavage peptide (called the γ peptide in FHV), which is probably a result of peptide–RNA recognition processes. Furthermore, mutagenesis of the autoproteolytic site of the capsomere yielded cleavage-incompetent FH virions. Although these particles were structurally indistinct from wild-type virions and packaged the correct RNA, they were not infectious (V. Reddy, A. Schneemann and J.E.J., unpublished observations), which suggests that cleavage of the γ sequence is required

Figure 1

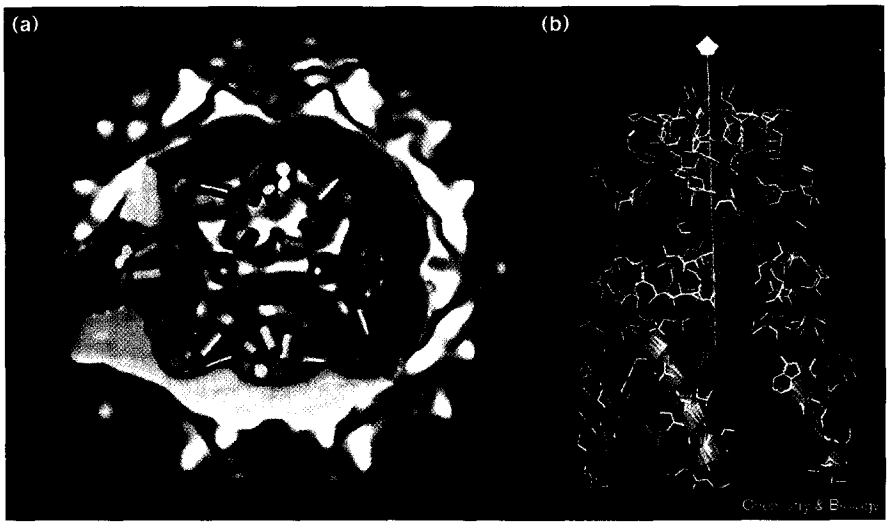

(a) A cut-away view of the whole Flock House virion, based on electron density derived from cryoEM reconstruction and X-ray structural data. The γ helices are represented as light blue cylinders along the C_5 axes; along the C_3 axes they are red and dark green. **(b)** A close-up view perpendicular to a C_5 axis, illustrating the helical-bundle formation of γ helices along this axis [8].

for infectivity. Additionally, matrix-assisted laser description/ionization mass spectroscopy (MALDI–MS) studies [11] on FHV have demonstrated that the γ peptide is readily accessible to tryptic digestion, indicating that the structural dynamics of the capsid assembly allow the sporadic presentation of the γ peptide on the exterior of the virus. These observations fueled the hypothesis [12] that these cleavage sequences play a dual role in nodaviral processes: the carboxy-terminal domain guides genome packaging, whereas the amino-terminal region serves to interact directly with the endosomal membrane to increase membrane permeability by disrupting lipid packing, allowing translocation of the viral genome (Figure 2).

We addressed the feasibility of the proposed function of the cleavage sequence by synthesizing the 21-residue Met→Nle (norleucine) variant of the amino-terminal helical domain of the γ peptide (designated γ_1) from FHV and evaluating its membrane activity against fluid-phase bilayers. Indeed, helical-wheel representation (Figure 3) of this sequence reveals considerable amphipathic character, a hallmark of many membrane-active peptides [13]. Liposome-based fluorescence experiments and ion-conductance measurements firmly establish the γ-peptide segment as a potent membrane-permeabilizing species and fluorescence and attenuated total reflectance infrared spectroscopy (ATR–IR) clearly delineate the mode of its lipid binding. The presence of negatively charged lipids in biomembranes led us to carry out our measurements on both zwitterionic and negatively charged phospholipids so as to understand the influence of electrostatics on peptide insertion and its consequent effects on membrane structure and permeability. The results describing the interaction of the γ peptide helical domain with fluid-phase lipids complement our prior studies [14] on the morphology-switching effects of γ_1 on gel-phase bilayers and further strengthen the hypothesis of cleavage-peptide-initiated RNA translocation in nodaviruses.

Figure 2

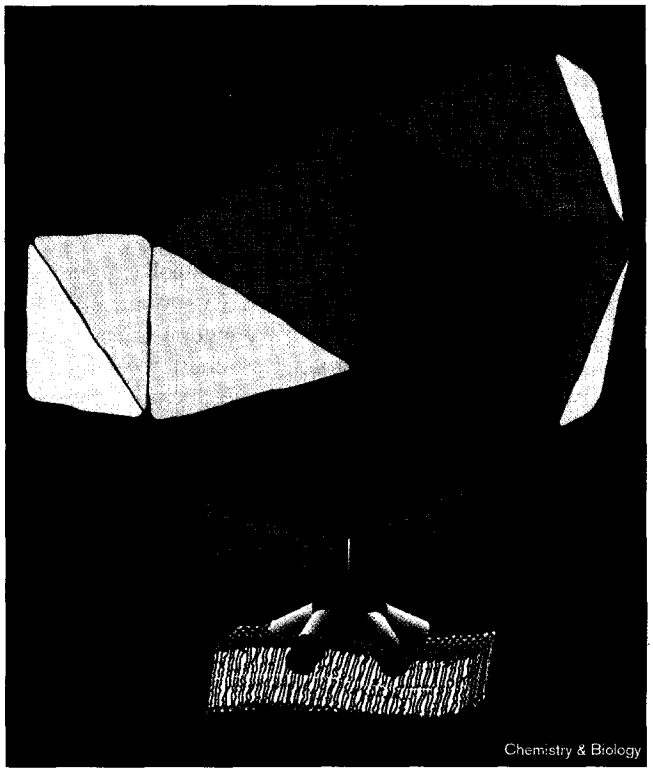

The release of the pentameric bundle of γ helices (shown in blue) along a C_5 axis of FHV (shown structurally abbreviated in green) and the subsequent insertion of the peptide bundle into a lipid membrane (yellow).

Figure 3

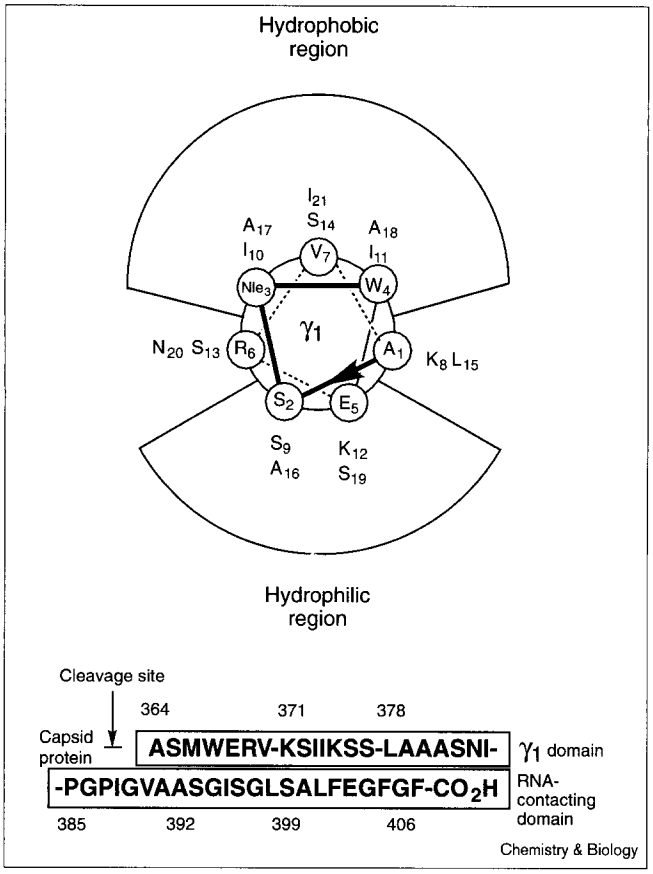

Helical-wheel representation of the amino-terminal 21 residues of the γ peptide. The γ_1 peptide used in these studies has a Met→Nle mutation. The numbered sequence of entire γ peptide is shown below, with the cleavage site indicated by an arrow and helical and RNA-contacting portions indicated in boxed regions.

Figure 4

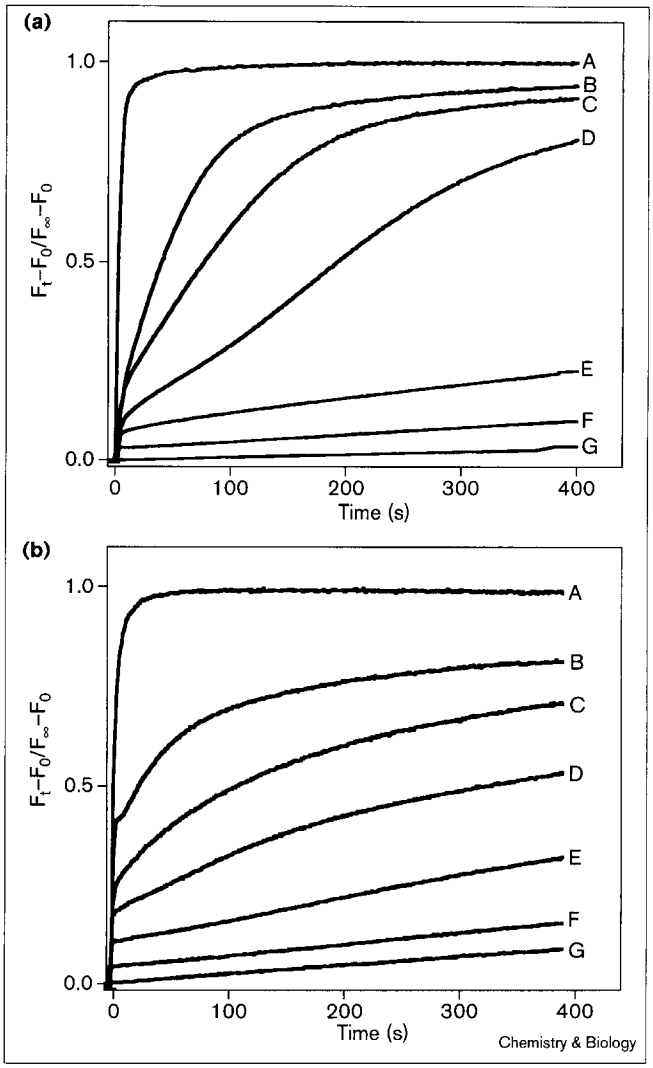

Time-dependent fluorescence traces describing the γ_1-induced release of 5(6)-carboxyfluorescein from **(a)** POPC and **(b)** POPG vesicles at varying lipid to peptide ratios. (a) A, 5:1; B, 19:1; C, 23:1; D, 31:1; E, 47:1; F, 93:1; G, 468:1. (b) A, 2:1; B, 4:1; C, 5:1; D, 7:1; E, 11:1; F, 21:1; G, 43:1.

Results

Dye release

Vesicles encapsulating (5)6-carboxyfluorescein (CF) dye at self-quenching concentration were prepared and used in an initial assay of the membrane activity of γ_1 [15]. Treating both zwitterionic 1-palmitoyl-2-oleoyl-*sn*-glycero-phosphocholine (POPC) and negatively charged 1-palmitoyl-2-oleoyl-*sn*-glycero-phosphoglycerol (POPG) vesicles with γ_1 results in a sharp increase in CF fluorescence, indicating leakage of dye from the liposomal compartment and dilution of CF dye into bulk solution (Figure 4). The fluorescence time trace displays similar kinetics for both lipids. Biphasic behavior is observed, with a high initial rate of increase upon addition of peptide followed by a much slower phase, which is peptide-concentration dependent. Interestingly, the negatively charged headgroups of POPG have the effect of augmenting membrane resistance to the γ_1 peptide. Significantly higher γ_1-peptide concentrations were necessary to induce dye release from POPG liposomes (lipid:peptide = 43:1) than from POPC liposomes (lipid:peptide = 468:1). The possibility of vesicle lysis as a mechanism for dye release was investigated by measuring both dynamic light scattering and 90° light scattering [16]. These experiments (data not shown) did not detect a significant change in size distribution of neutral POPC liposomes upon treatment with peptide, suggesting that the percentage of vesicles lysed or fused, if at all, is low in the concentration range of our measurements. The addition of γ_1 to POPG large unilamellar vesicles (LUVs) at a 47:1 lipid to peptide ratio altered the light scattering significantly, suggesting that the positively charged γ_1 might be inducing aggregation of the negatively charged POPG vesicles. Accordingly, a strong peptide interaction with the negatively charged phosphoglycerol headgroup could be

Figure 5

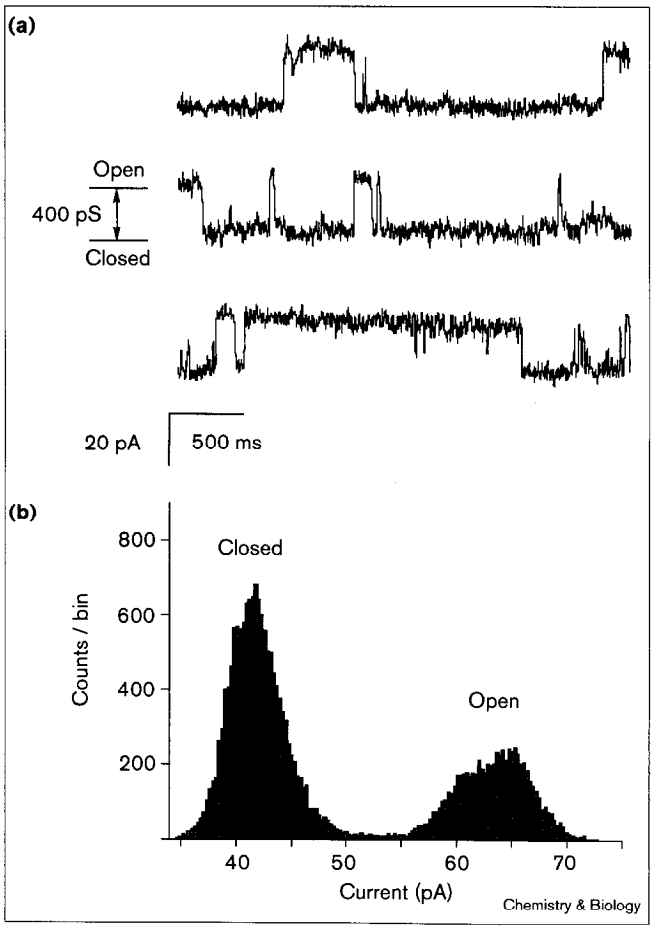

Conductance trace induced by γ_1 obtained using the pipette tip-dip method with planar lipid bilayers composed of soybean lecithin separating symmetric 500 mM KCl salt solutions. **(a)** A continuous trace at 50 mV holding potential. **(b)** The statistical distribution of conductance states is shown. Each bin represents a 0.3 pA range. The difference in current between the centers of each peak represents the 20 pA current passed in the predominant open state. During this burst of channel activity, the channel is in the open state 35% of the time and is considered to be in the closed state the remainder of the time.

acting to localize the peptide at the headgroup region, thereby preventing the same extent of bilayer penetration as in POPC LUVs, which would decrease the efficacy of dye release from POPG liposomes.

Single-channel ion conductance

Evidence for the formation of transmembrane channels by γ_1 was provided by ion-conductance measurements across planar lipid bilayers bathed on either side with buffered, symmetric salt solutions using the pipette tip-dip method [17]. Application of potential across the bilayer allowed the voltage-driven ion current induced by γ_1 upon its bilayer partitioning to be measured. Although multiple conductance states were observed, periods of single-channel-type conductance on the order of seconds were obtained with γ_1, in which there was a predominant 460 pS gated conductance state (Figure 5). Although the uniform open-state conductance values observed in the current traces are consistent with the formation of a discrete pore rather than a gross structural disruption in the membrane, the oligomerization state causing current flow is unclear. One can, however, make a rough approximation of the nature of the conducting state: a 460 pS conductance corresponds to 7 Å effective pore diameter if one assumes that the peptide forms a cylindrical water-filled transmembrane channel in which ion conductances are similar to those in bulk solution [18]. This estimated relationship between conductance and pore size compares favorably with that obtained for other channel-forming peptides [19]. If one further assumes a helical barrel stave model for the channel species, then a geometrical analysis suggests a oligomerization state between 5 and 7. Indeed, structural examination of FHV places the γ peptide in a helical-bundle arrangement with its symmetry-related partners along the C_5 axes of the virion — it is therefore tempting to invoke the pentameric bundle as an active channel-forming oligomer. The hypothesized delivery of the γ peptide to its target membrane is thought to occur via expulsion of the cleavage sequence from the viral interior along the C_5 symmetry axes. Certainly, the considerable conductance induced by γ_1 across planar lipid bilayers provides clear evidence of the ability of γ_1 to dramatically increase membrane permeability upon insertion.

Structure of the peptide–lipid complex

Tryptophan fluorescence measurements

Peptide incorporation into fluid bilayers was further probed using vesicles containing lipids functionalized with radical fluorescence quenchers. Liposomes were prepared that contained varying concentrations of lipids functionalized with doxyl groups and normal phospholipids. Depth of γ_1 penetration was determined by the parallax method using the fluorescence of Trp4 as a label. Monitoring static fluorescence quenching by doxyl nitroxide quenchers covalently bound at the C_5 and C_{10} positions of the dopant lipid acyl chains allowed the distance of the fluorophore from the bilayer center to be determined using the following equation:

$$\frac{F}{F_0} = \exp\left[-\pi\left(\frac{c}{A}\right)(R^2 - X^2 - Z^2)\right] \quad (1)$$

where F and F_0 are the fluorescence intensities with and without quencher, respectively, c is the mole fraction of nitroxide-quencher-modified lipids, A is the lipid longitudinal cross-sectional area, R is the hardsphere critical quenching radius, X is the closest quencher to fluorophore lateral distance and Z is the closest quencher to fluorophore vertical distance [20]. A plot of $\ln(F/F_0)$ against mole fraction χ of quencher lipid (Figure 6) reveals the

Figure 6

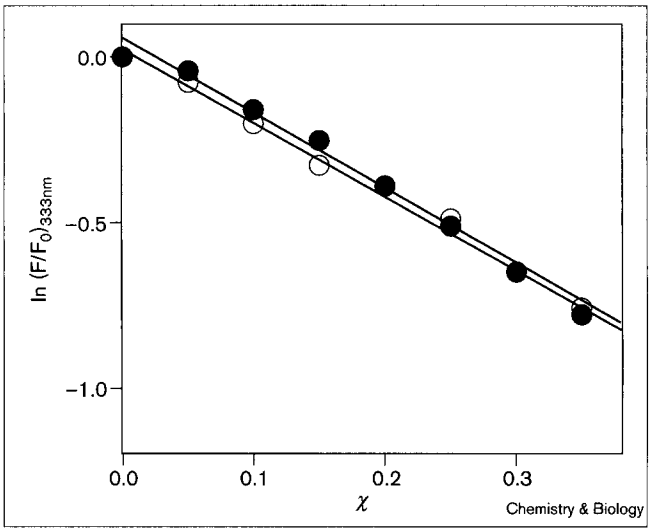

Fluorescence intensity of Trp4 of membrane-bound γ_1 peptide, as affected by increasing mole fraction (χ) of nitroxide quenchers. ○, 1-palmitoyl-2-stearoyl(5-DOXYL)-*sn*-glycero-3-phosphocholine; ●, 1-palmitoyl-2-stearoyl(10-DOXYL)-*sn*-glycero-3-phosphocholine in POPC bilayers. The solid lines are linear regressions with the following slopes: ○, 2.3 ± 0.1 and ●, 2.17 ± 0.08.

Figure 7

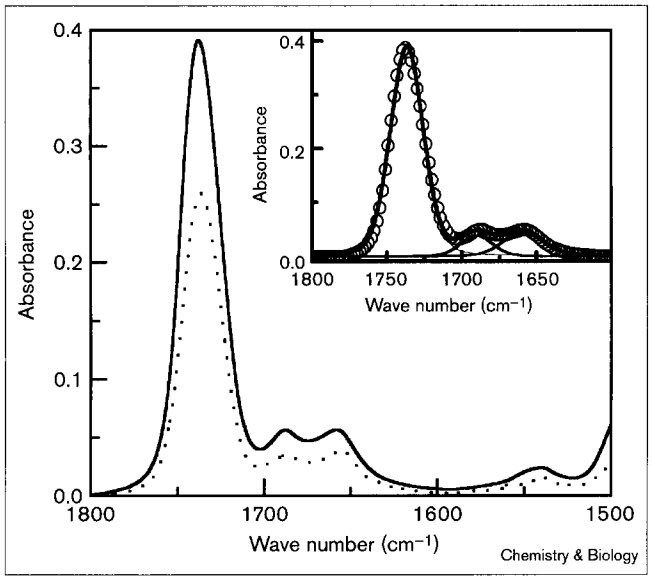

ATR–FT–IR spectra of γ_1 in POPC multibilayers (peptide to lipid ratio of 1:150) on a germanium crystal. The solid line is the absorbance with incident light plane-polarized parallel to the surface normal and the dotted line is that with perpendicularly polarized light. The inset displays the band decomposition of the parallel component with mixed Lorentzian/Gaussian functions (thin lines, 0.5:0.5) with the component sum displayed as a thick line with circles. The peak areas were obtained by integrating the component peaks.

expected linear relationship, allowing calculations [21] that position the Trp4 of γ_1 ~10 Å from the bilayer midplane.

ATR–FT–IR measurements

The molecular orientation of γ_1 peptides relative to Trp4 in dried γ_1-lipid multibilayers was examined using ATR–IR spectroscopy. Preformed complexes of peptide with both POPC and POPG liposomes were dried on a germanium ATR crystal at a lipid to peptide ratio of 150:1. Orientation information relative to the supporting surface was extracted from the ratio of IR absorption intensities (dichroic ratio) observed with light polarized parallel and perpendicular to the germanium surface using known methods [22,23]. Comparison of these spectra with those of pure lipids revealed negligible differences in the lipid IR absorbance regions, suggesting that the peptide does not appreciably alter bilayer lipid orientation in this concentration range. In both analyses, the IR dichroic ratio of the lipid symmetric CH_2 vibrational band (R_{2850}) was 1.08 ± 0.7, which indicates a 28 ± 1° angle between the lipid chain and the surface normal. Peptide orientation was determined independently from IR dichroism of the amide I band (consisting primarily of the C=O stretch, 1656 cm^{-1}) in the lipid complex (Figure 7). The lipid-bound cleavage sequence exhibited an amide I dichroic ratio (R_{1656}) between 1.3 and 1.6; similarly, in POPG-peptide multibilayers, the amide I dichroic ratio was between 1.1 and 1.7. After correcting for the influence of the 70% α-helical content measurements from circular dichroism (CD) measurements on dried peptide–lipid multibilayers (data not shown), the order parameters locate the peptide helical axis at a 66°–78° angle from the surface normal when complexed with POPC and at a 62°–90° angle in POPG. Despite significant differences in permeability effects, as well as association enthalpies (D.T.B, A.J., C.S. and M.R.G, unpublished observations), the bound peptide orientation is approximately the same in both negatively charged and neutral lipid bilayers (Figure 8).

Discussion

Biophysical studies have shown the γ_1 peptide to be a highly membrane-active species that binds avidly to fluid phase lipid bilayers (D.T.B, A.J., C.S. and M.R.G, unpublished observations) and increases transmembrane permeability. Fluorescence quenching data and ATR–IR analysis of peptide–lipid complexes place this helical region of the FHV cleavage sequence ~1 nm from the bilayer midplane, with its helical axis roughly perpendicular to the membrane surface normal: only half of the peptide surface packs against the lipid matrix, whereas the other half remains solvent exposed, as expected for an amphiphilic helix. These results are consistent with our related thermodynamic studies (D.T.B, A.J., C.S. and M.R.G, unpublished observations) on γ_1-membrane partitioning, which revealed partitioning free energies of approximately −7.5 kcal/mol for both POPC and POPG membranes, corresponding to hydrophobic burial of half of the surface area of a 21-residue α helix.

Figure 8

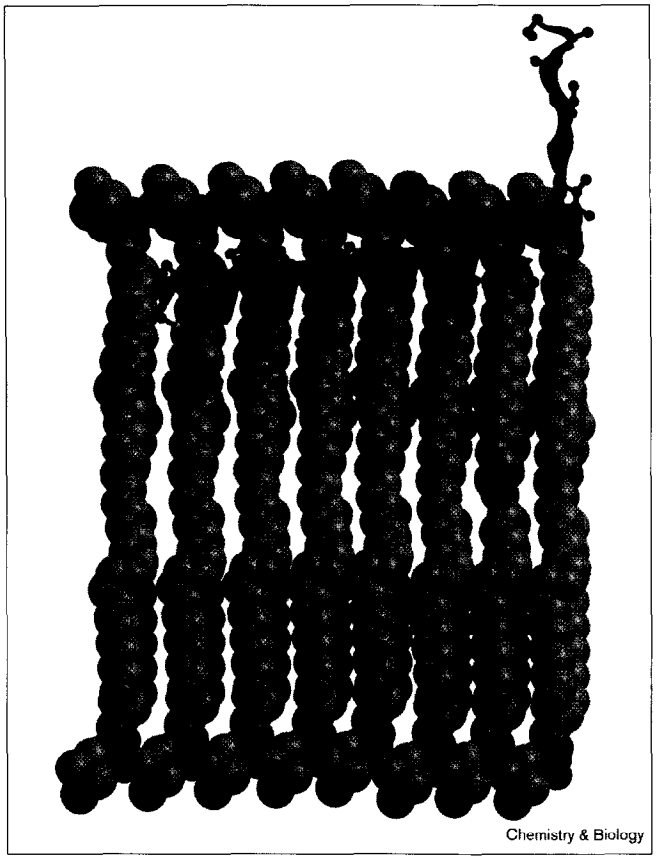

A schematic depiction of the peptide–lipid complex, on the basis of our biophysical data. The γ_1 peptide is shown as a green helix with sidechains rendered in ball-and-stick style and incorporated into a POPC bilayer at a 72° angle from the bilayer normal. The lipid tilt is at an angle of 28° into the plane of the figure. The carboxy-terminal residues of the γ peptide sequence that were not synthesized are shown in blue. POPC lipids are rendered as space-filling structures in which carbon is grey, oxygen is red, nitrogen is blue and phosphorous is purple. Hydrogen atoms have been omitted for clarity. These images were generated using the MOLSCRIPT interface with Raster3D [30,31].

Certainly, one can easily envision membrane partitioning occurring in this fashion when the γ peptide becomes externalized on the virion surface (Figure 2). The helical region is expected to end prior to a PGP (proline–glycine–proline) sequence (Figure 3), which could serve as a turn element, facilitating bilayer incorporation of the γ_1 sequence (Figure 8).

Enhanced permeability demonstrated by fluorescence studies proceeds without significant membrane lysis or fusion, which suggests that the γ-peptide–membrane interaction leads to either the formation of discrete pores or wide-spread disruption of lipid packing. Although the structural model (Figure 8), constructed from the aforementioned studies, seems to preclude discrete pore formation, these processes in general are not mutually exclusive but rather competing, concentration-dependent processes. Channel recordings obtained with the γ-peptide segment provide evidence for the formation of a discrete channel, whereas the substantial 460 pS conductance reflects the large disruptions implied by dye leakage [19]. The preponderance of single-channel-type events observed in the recordings suggests a preferred oligomerization state rather than indiscriminate aggregation or bilayer destruction, although the actual nature of the bilayer-inserted species is unclear under these circumstances. Voltage-clamped conditions of the ion-conductance measurements are distinct from those of the liposome experiments, and therefore the peptide insertion behavior is probably different [21,24–26]. Certainly, insertion orientation can be highly dependent on peptide–lipid ratios as well as degrees of lipid hydration. Both analyses share the common result that the viral cleavage sequence γ_1 drastically compromises membrane integrity, however, a key finding with regard to the hypothesis of cleavage-peptide-mediated viral genome translocation.

The existence of such a lipophilic domain in the cleavage sequence of FHV provides compelling support for its proposed role as a membrane-permeabilizing agent in the viral RNA translocation process. Liberation of endosomal virions demands membrane rupture of some kind, and the γ_1 sequence has an exceptional capability to deliver the requisite activity. Indeed, this sequence-encoded permeabilizing function of the amino-terminal γ domain complements the previously established role of the carboxy-terminal γ domain in controlling genome recognition and packaging. It stands to reason that the selection pressures driving development of the minimal nodavirus system would also implement multifunctionality within each gene product. The present data support the hypothesis that release of nodaviral particles from the endosome proceeds via expulsion of the lipophilic γ domains from the capsid interior into the endosomal membrane, where it creates a local disruption of bilayer structure (Figure 2), allowing RNA delivery into the host cytoplasm. Although one expects that protonation of the amine functionalities on the γ peptide at lowered endosomal pH would prevent efficient membrane partitioning, related studies (D.T.B, A.J., C.S. and M.R.G, unpublished observations) have shown that the membrane partition constant of γ_1 decreases only slightly when the pH is decreased from 7.0 to 4.5. This minor decrease in lipophilicity is expected to be offset by enhanced externalization (and therefore increased membrane concentration) of the noncovalently bound peptide resulting from destabilization of the viral assembly at lowered pH. Externalization of membrane-binding hydrophobic capsid domains of nonenveloped viruses has been documented in studies of poliovirus infection mechanisms [2]. Furthermore, resonance of the helical-bundle motif of cleavage peptides in the structures of related nonenveloped viruses [27] suggests a conserved biological function of this construct. Additionally,

although the cleavage peptide sequence is not conserved, the hydrophobic patterning near the amino terminus bears similarities across virus families [9,27], further suggesting functional conservation. These observations, coupled with the data presented here, which testify to the acute membrane activity of γ_1, serve to implicate the γ peptide in a crucial membrane-permeabilizing event central to the transfection process.

Significance

Transmembrane passage of nonenveloped viruses or genome translocation must occur through the intermediacy of virus–membrane-protein interactions, or direct protein–lipid interactions. We have identified a highly membrane-active peptide sequence, γ_1, in a nonenveloped RNA animal virus, known as the Flock House nodavirus (FHV). This peptide sequence (with a Met→Nle mutation) represents the amino-terminal 21 residues of the 44-residue γ peptide, which is cleaved from the carboxyl terminus of the FHV capsid protein in an autocatalytic proteolysis event that is essential for viral infectivity. Previous research has revealed the following about FHV: infectivity is contingent upon the post-assembly autocatalytic cleavage of the γ peptide; γ is located at the high symmetry axes of the virion, a probable point of rupture and release of RNA; and similar cleavage peptide structural motifs have been found in other nonenveloped viruses. We report here a complete description of γ_1–lipid interactions using a number of biophysical methods and have established the propensity of γ_1 for spontaneous partitioning into lipid bilayers concomitant with large increases in membrane permeability.

Together the *in vivo* and structural observations and the results of the present *in vitro* study implicate the cleavage peptide in direct protein–lipid interactions that could effect viral genome translocation across the endosomal membrane. These results support the mechanistic hypothesis of nodaviral infection in which receptor binding destabilizes viral assembly, allowing the delivery of a membrane-disrupting agent (in this case, the γ peptide) to the target membrane, which subsequently permeabilizes the bilayer to the viral genome. We postulate that selectivity is governed by a specific virus–receptor interaction that is coupled to a nonspecific interaction of the cleavage peptide with the membrane, which induces membrane disruption and transmembrane passage of viral material. These results therefore validate further *in vivo* examination of the role of the nodaviral cleavage sequences in the transfection process.

Materials and methods

Materials

1-Palmitoyl-2-oleoyl-sn-glycero-3-phosphocholine (POPC) and 1-palmitoyl-2-oleoyl-sn-glycero-3-phosphoglycerol (POPG) were purchased from Avanti Polar Lipids, AL. Methanol and chloroform were of high-performance liquid chromatography (HPLC) and optima grade respectively, and were obtained from Fisher Scientific. Boc-amino acids were used as obtained from Novabiochem, as was hydroxybenzotriazole. All lipids and solvents were used as purchased without further purification.

Peptide synthesis

Manual Boc solid-phase peptide synthesis was carried out according to the *in situ* neutralization protocol of Kent [28] with HBTU activation on methylbenzhydrylamine (MBHA) resin (0.56 mequiv/g loading). Formyl protection on tryptophan was removed prior to resin cleavage by treatment of the peptide with 10% hydrazine monohydrate in dimethyl formamide (DMF) at 0°C for 8 h. Peptides were cleaved from resin using standard hydrofluoric acid (HF) procedures (10 ml 8:1:0.5:0.5 HF/anisole/thiophenol/dimethylsulfide per gram of peptide resin; 2 h at 0°C) and eluted from the resin with trifluoroacetic acid (TFA) following washing with ethyl ether. The resulting free peptide solution was lyophilized, redissolved in acidic water/acetonitrile and purified using reverse-phase HPLC on a Vydac C_{18} column using a CH_3CN/H_2O/TFA gradient. The isosteric substitution of Met→Nle was made to obviate problems with thioether oxidation, and thus all measurements are done with the γ_1 peptide, which bears this substitution.

Liposome preparation

Lipids were used as purchased to prepare films by drying the lipid dissolved in chloroform under a stream of nitrogen while heating followed by several hours under vacuum. Multilamellar vesicles were prepared by swelling the lipid film in buffer while incubating at 65°C for 30 min with periodic vortexing for 30 s. Vesicles for ATR–IR measurements were prepared in doubly-deionized water. The resulting multilamellar vesicles were then sized at 65°C by extrusion through stacked polycarbonate membranes with pore diameters of approximately 200 nm using a miniextruder (LiposoFast, Avestin) to obtain large unilamellar vesicles (LUVs). Lipid concentration was determined after extrusion by lyophilization of a known volume of the LUV suspension and analysis of the resulting powder by ^1H NMR in $CDCl_3$, using dioxane or benzene as an internal standard for peak integration. An acquisition delay of 15 s was used to ensure integration accuracy. Peptide concentration was determined using UV spectroscopy assuming an extinction coefficient of 5570 $cm^{-1}M^{-1}$ at 280 nm.

CF release assay

Measurements were performed in 100 mM Tris, 200 mM NaCl, pH 7.0 at 25°C. A self-quenching (50 mM) solution of 5(6)-carboxyfluorescein (CF) was entrapped in POPC LUVs and the resulting LUVs were separated from nonincorporated dye by gel filtration. The time resolved release of CF from large unilamellar vesicles was determined by monitoring the fluorescence intensity F_t at an emission wavelength of 520 nm with excitation at 490 nm and 4 nm bandpass in a cuvette containing 2 ml of 2–8 mM phospholipid in 100 mM Tris, 200 mM NaCl, pH 7.0. The stirred solution was equilibrated for 5 min at 25°C before starting the experiment. Release was initiated by injecting 5–25 ml of peptide stock solution and the total fluorescence intensity F_∞ was determined at the end of the experiment by adding 100 ml of 10% Triton X-100 and correcting for dilution. The relative change in fluorescence intensity is reported as $F_t-F_\infty/F_0-F_\infty$, where F_0 denotes the initial fluorescence intensity. Control experiments were performed by adding pure DMSO and gramicidin dissolved in dimethyl sulfoxide (DMSO) in order to ensure that vesicles do not release dye upon addition of these compounds.

Channel conductance measurements

Micropipettes were pulled on a Flaming/Brown micropipette puller, model P-87 from Sutter Instruments. Open resistances were consistently between 5 and 10 MΩ. Membrane voltage was controlled and currents were measured and detected using an Axopatch 1-D patch clamp amplifier (Axon Instruments), a low-pass Bessel filter (Frequency Devices), Digidata 1200 digital/analog converter interface (Axon Instruments), and a Tektronix 466 storage oscilloscope. Planar lipid

bilayers were formed on micropipette electrodes using Type II-S soybean phosphatidylcholine (Sigma). Bilayers formed ranged from 1 to 20 GΩ resistance. In a typical experiment, a 5 µl aliquot of peptide solution (1 mM in H_2O) was added to 150 µl subphase buffer (symmetrical salt conditions; 500 mM KCl, 5 mM $CaCl_2$, 10 mM HEPES, pH 7.5), resulting in spontaneous partitioning of peptide into the lipid bilayer. Channel activity appeared within 4 min of peptide addition. Data acquisition and analysis was performed using the pClamp6 software package (Axon Instruments). Estimates of pore diameter were made using the Nernst–Einstein equation relating the diffusion coefficient D (in this case the diffusion coefficient of potassium in water) to l, the ionic conductivity:

$$\lambda = \frac{z^2F^2D}{RT} \quad (2)$$

where *z*, *F*, *R* and *T* are ionic charge, Faraday's constant, the universal gas constant and temperature in degrees Kelvin, respectively. Ionic conductivity has units of siemens × cm^2 × mol^{-1}, and thus the product of λ, ion concentration (*C*) and the ratio of cross-sectional channel area (*A*) to channel length (*d*) provides a theoretical estimate of the channel conductance [18].

Light scattering

The intensity of light scattered by vesicles at 90° to the incident beam before and after addition of peptide was measured on an Aminco/Bowman luminescence spectrometer equipped with a water-jacketed sample chamber thermostatted at 25°C using an incident wavelength of 400 nm and 4 nm bandpass.

FT–ATR–IR spectroscopy

Oriented lipid multibilayers were prepared by drying 500 ml of DPPC–LUV–peptide suspension (lipid concentration: 1 mg/ml, lipid to peptide ratio of 150:1) on a germanium crystal ($\theta = 45$, Spectra-Tech) under nitrogen atmosphere. Spectra were acquired under dry nitrogen atmosphere at 4 cm^{-1} resolution on a Nicolet 550 Magna Series II FT–IR instrument equipped with a liquid nitrogen cooled mercury–cadmium telluride detector. A baseline horizontal ATR optical bench holding the germanium crystal (Spectra-Tech) and a ZnSe polarizer (Spectra-Tech) were implemented in the spectrometer. Reported spectra are the average of 800 scans taken with light polarized either parallel or perpendicular to the germanium surface normal.

Calculation of orientation

IR dichroism of peptide amide I (1656 cm^{-1}, C=O stretch) and lipid symmetric CH2 (2850 cm^{-1}) stretching vibrations were used to gauge molecular orientation in each sample. In addition, amide bond vibrational frequencies in the region of 1700–1500 cm^{-1} and 3200–3500 cm^{-1} were also used as diagnostic measures of peptide secondary structure. The maximum intensities of the amide I and amide II (primarily amide N–C stretch) bands were observed at 1656 cm^{-1} (1684, 1656 cm^{-1}) and at 1546 cm^{-1} (1532, 1547 cm^{-1}), respectively. The numbers in brackets refer to the decomposition of the vibrational peaks by fitting mixed Lorentzian/Gaussian (0.5:0.5) functions to the data. Peak areas were determined by integrating the subsequent peak fit. The observed amide A (amide NH stretching) band appearing at 3293 cm^{-1} indicates hydrogen bonding. Orientation information was extracted from dichroic ratios according to published methods [23]. Briefly, the dichroic ratio R is defined as the ratio of absorption obtained with incident light plane-polarized parallel to the surface normal ($A_{\parallel}$) to that obtained with light plane-polarized perpendicular to the surface normal ($A_{\perp}$). The angle α between the α-helix axis and the transition dipole moment of the amide I transition was assumed to be 39°, whereas the angle between the lipid CH_2.transition dipole moment and the lipid chain axis was set to 90° [29]. One can then calculate the angle between the surface normal and the molecular axis of the α helix while correcting for the helical content of γ_1, as determined using CD.

Fluorescence measurements

All fluorescence emission measurements were performed on an Aminco/Bowman luminescence spectrometer equipped with a water-jacketed sample chamber thermostatted at 25°C. Each spectrum was background corrected (buffer and vesicle light scattering). Tryptophan fluorescence was monitored from 300–450 nm with excitation at 280 nm and 4 nm bandpass through a 300 nm low pass filter (Hoya Optics). Experiments probing the efficiency of collisional quenching of tryptophan by CsCl were performed as previously described [14]. Static quenching experiments from the lipid phase were performed using large unilamellar vesicles composed of POPC and either 1-palmitoyl-2-stearoyl(5-DOXYL)-*sn*-glycero-3-phosphocholine or 1-palmitoyl-2-stearoyl-(10-DOXYL)-*sn*-glycero-3-phosphocholine (0–35 mole percent). The lipid to peptide ratio was 150:1 in all samples.

Acknowledgements

We thank the Skaggs Institute for Chemical Biology for the primary financial support of this program and also the Fonds der Chemische Industrie (A.J.) and the DFG (C.S.) for postdoctoral fellowships.

References

1. Schneemann, A., Reddy, V. & Johnson, J.E. (1998). The structure and function of nodavirus particles: a paradigm for understanding chemical biology. *Adv. Virus Res.* **50**, 381-446.
2. Fricks, C.E. & Hogle, J.M. (1990). Cell-induced conformational change in poliovirus: externalization of the amino terminus of VP1 is responsible for liposome binding. *J. Virol.* **64**, 1934-1945.
3. Casasnovas, J.M. & Springer, T.A. (1994). Pathway of rhinovirus disruption by soluble intercellular adhesion molecule 1 (ICAM-1): an intermediate in which ICAM-1 is bound and RNA is released. *J. Virol.* **68**, 5882-5889.
4. Rossmann, M.G. (1994). Viral cell recognition and entry. *Protein Sci.* **3**, 1712-1725.
5. Schneemann, A., Zhong, W., Gallagher, T.M. & Rueckert, R.R. (1992). Maturation cleavage required for infectivity of a nodavirus. *J. Virol.* **66**, 6728-6734.
6. Zlotnick, A., *et al.*, & Johnson, J.E. (1994). Capsid assembly in a family of animal viruses primes an autoproteolytic maturation that depends on a single aspartic acid residue. *J. Biol. Chem.* **269**, 13680-13684.
7. Hosur, M.V., *et al.*, & Rueckert, R.R. (1987). Structure of an insect virus at 3.0 Å resolution. *Proteins* **2**, 167-176.
8. Cheng, R.H., Reddy, V.S., Olson, N.H., Fisher, A.J., Baker, T.S. & Johnson, J.E. (1994). Functional implications of quasi-equivalence in a T = 3 icosahedral animal virus established by cryoelectron microscopy and X-ray crystallography. *Structure* **2**, 271-282.
9. Munshi, S., *et al.*, & Johnson, J.E. (1996). The 2.8 Å structure of a T = 4 animal virus and its implications for membrane translocation of RNA. *J. Mol. Biol.* **261**, 1-10.
10. Schneemann, A. & Marshall, D. (1998). Specific encapsidation of nodavirus RNAs is mediated through the C terminus of capsid precursor protein alpha. *J. Virol.* **72**, 8738-8746.
11. Bothner, B., Dong, X.F., Bibbs, L., Johnson, J.E. & Siuzdak, G. (1998). Evidence of viral capsid dynamics using limited proteolysis and mass spectrometry. *J. Biol. Chem.* **273**, 673-676.
12. Fisher, A.J. & Johnson, J.E. (1993). Ordered duplex RNA controls capsid architecture in an icosahedral animal virus. *Nature* **361**, 176-179.
13. Lear, J.D., Wasserman, Z.R. & DeGrado, W.F. (1988). Synthetic amphiphilic peptide models for protein ion channels. *Science* **240**, 1177-1181.
14. Janshoff, A., Bong, D.T., Steinem, C., Johnson, J.E. & Ghadiri, M.R. (1999). An animal virus-derived peptide switches membrane morphology: possible relevance to nodaviral transfection processes. *Biochemistry,* **38**, 5328-5336.
15. Weinstein, J.N., Klausner, R.D., Innerarity, T., Ralston, E. & Blumenthal, R. (1981). Phase transition release, a new approach to the interaction of proteins with lipid vesicles. Application to lipoproteins. *Biochim. Biophys. Acta* **647**, 270-284.
16. Grant, E., Jr., Beeler, T.J., Taylor, K.M. P., Gable, K. & Roseman, M.A. (1992). Mechanism of magainin 2a induced permeabilization of phospholipid vesicles. *Biochemistry* **31**, 9912-9918.
17. Suarez-Isla, B.A., Wan, K., Lindstrom, J. & Montal, M. (1983). Single-channel recordings from purified acetylcholine receptors reconstituted in bilayers formed at the tip of patch pipets. *Biochemistry* **22**, 2319-2323.

18. Stein, W.D. (1986). *Transport and Diffusion Across Membranes.* Academic Press, Orlando, Florida.
19. Smart, O.S., Breed, J., Smith, G.R. & Sansom, M.S.P. (1997). A novel method for structure-based prediction of ion channel conductance properties. *Biophys. J.* **72**, 1109-1126.
20. Birks, J.B. (1970). *Photophysics of Aromatic Molecules.* (Wiley Monographs in Chemical Physics), Wiley-Interscience, New York.
21. Chung, L.A., Lear, J.D. & DeGrado, W.F. (1992). Fluorescence studies of the secondary structure and orientation of a model ion channel peptide in phospholipid vesicles. *Biochemistry* **31**, 6608-6616.
22. Tamm, L.K. (1994). Physical studies of peptide-bilayer interactions. In *Membrane Protein Structure.* (White, S. ed.) Oxford University Press, New York, 283-313.
23. Tamm, L.K. & Tatulian, S.A. (1997). Infrared spectroscopy of proteins and peptides in lipid bilayers. *Q. Rev. Biophys.* **30**, 365-429.
24. Archer, S.J., Ellena, J.F. & Cafiso, D.S. (1991). Dynamics and aggregation of the peptide ion channel alamethicin. Measurements using spin-labeled peptides. *Biophys. J.* **60**, 389-398.
25. Skerjanc, I.S., Shore, G.C. & Silvius, J.R. (1987). The interaction of a synthetic mitochondrial signal peptide with lipid membranes is independent of transbilayer potential. *EMBO J.* **60**, 3117-3123.
26. Stankowski, S., Pawlak, M., Kaisheva, E., Robert, C.H. & Schwarz, G. (1991). A combined study of aggregation, membrane affinity and pore activity of natural and modified melittin. *Biochim. Biophys. Acta* **1069**, 77-86.
27. Kaesberg, P., *et al.*, & Johnson, J.E. (1990). Structural homology among four nodaviruses as deduced by sequencing and X-ray crystallography. *J. Mol. Biol.* **214**, 423-435.
28. Schnolzer, M., Alewood, P., Jones, A., Alewood, D. & Kent, S.B.H. (1992). *In situ* neutralization in Boc-chemistry solid phase peptide synthesis. Rapid high yield assembly of difficult sequences. *Int. J. Pept. Protein Res.* **40**, 180-193.
29. Frey, S. & Tamm, L.K. (1991). Orientation of melittin in phospholipid bilayers. A polarized attenuated total reflection infrared study. *Biophys. J.* **60**, 922-930.
30. Kraulis, P.J. (1991). MOLSCRIPT: a program to produce both detailed and schematic plots of protein structures. *J. Appl. Crystallogr.* **24**, 946-950.
31. Merritt, E.A. & Murphy, M.E.P. (1994). Raster3D version 2.0. A program for photorealistic molecular graphics. *Acta Crystallogr. D* **50**, 869-873.

Because *Chemistry & Biology* operates a 'Continuous Publication System' for Research Papers, this paper has been published via the internet before being printed. The paper can be accessed from http://biomednet.com/cbiology/cmb – for further information, see the explanation on the contents pages.